A New Framework to Estimate Breathing Rate from Electrocardiogram, Photoplethysmogram, and Blood Pressure Signals

ALI ADAMI[1], REZA BOOSTANI[2], FAEZEH MARZBANRAD[3], AND PETER H. CHARLTON.[4],

[1]School of Electrical and Computer Engineering Shiraz University, Shra, Iran (e-mail: ali.adm71@gmail.com)
[2]School of Electrical and Computer Engineering Shiraz University, Fars, Iran (e-mail: r.boostani@gmail.com)
[3]Department of Electrical and Electronic Engineering, Monash University, Melbourne, Australia (e-mail: faezeh.marzbanrad@monash.edu)
[4]Department of Public Health and Primary Care, University of Cambridge, Cambridge, United Kingdom (e-mail: pc657@medschl.cam.ac.uk)

Corresponding author: Faezeh Marzbanrad (e-mail: faezeh.marzbanrad@monash.edu).

ABSTRACT Breathing Rate (BR) is a key physiological parameter measured in a wide range of clinical settings. However, it is still widely measured manually. In this paper, a novel framework is proposed to estimate the BR from an electrocardiogram (ECG), a photoplethysmogram (PPG), or a blood pressure (BP) signal. The framework uses Empirical Mode Decomposition (EMD) and Discrete Wavelet Transform (DWT) methods to extract respiratory signals, taking advantage of both time and frequency domain information. An Extended Kalman Filter (EKF), incorporating a Signal Quality Index (SQI), enabled our method to achieve acceptable performance even for significantly distorted periods of the signals. Using state vector fusion, the output signals are combined and finally the BR is estimated. The framework was tested on two publicly available clinical databases: the MIT-BIH Polysomnographic and BIDMC databases. Performance was evaluated using the mean absolute percentage error (MAPE). The results indicated high accuracy: MAPEs on the two databases of 3.9% and 3.6% for ECG signals, 6.0% for PPG, and 5.0% for BP signals. The results also indicated high robustness to noise down to $0dB$. Therefore, this framework may have utility for BR monitoring in high noise settings.

INDEX TERMS Breathing rate (BR), electrocardiogram (ECG), photoplethysmogram (PPG), blood pressure (BP), respiratory rate, respiratory signals, empirical mode decomposition (EMD), discrete wavelet transform (DWT).

I. INTRODUCTION

BREATHING Rate (BR) is a valuable physiological marker measured from patients in a wide range of settings including emergency departments, intensive care units and hospital wards. BR has been shown to be a sensitive indicator of patient deterioration. For instance, elevated BRs may precede cardiac arrest or respiratory dysfunction [1]. BR can also be used as a predictive index of in-hospital mortality [2]. In addition, BR is used in the diagnosis of several diseases such as pneumonia and sepsis [3]. Sensors are available for direct respiratory monitoring based on techniques such as spirometry, pneumography or plethysmography. However, these sensors can influence breathing patterns and can be obtrusive, and so their use is limited to specific clinical scenarios such as stress testing and sleep apnea diagnosis

[4]. Less obtrusive respiratory monitoring techniques may be more acceptable to patients, and consequently could be used in a wider range of clinical settings.

Breathing can influence several commonly monitored physiological signals such as the electrocardiogram (ECG), the photoplethymogram (PPG), and the blood pressure (BP) signal. Physiological mechanisms of respiration can modulate ECG, PPG, and BP signals in three different ways: baseline wander (BW), amplitude modulation (AM) and frequency modulation (FM) [5], [6]. Consequently, a wide range of algorithms have been proposed to extract respiratory signals from ECG, PPG, and BP signals, and to subsequently estimate BR, as reviewed in [7].

In this paper, we present a new framework to estimate BR from ECG, PPG, and BP signals. The engineering techniques

used in this framework are now introduced. The Discrete Wavelet Transform (DWT) and Empirical Mode Decomposition (EMD) can be used to decompose a signal into a set of signals, allowing one to extract a respiratory signal (herein referred to as ECG-Derived Respiration (EDR), PPG-Derived Respiration (PDR), or BP-Derived Respiration (BDR) signals [8]). They have been widely applied to ECG signals [9], [10]. Since EMD and DWT methods are not absolutely superior to each other, we have used both of them simultaneously to improve the performance of the estimator. Having obtained a respiratory signal, Power Spectral Density (PSD), a measure of a signal's power across the range of frequency content, has been widely used to estimate BR [3], [4]. The Welch periodogram is a technique for estimating the PSD [11] which averages power spectra calculated from shorter segments of the input signal to provide increased robustness to noise. PSD is widely used in algorithms to estimate BR, such as from ECG and PPG signals measured during exercise in [12] and [13], respectively.

A signal quality index (SQI) is an index or algorithm used to assess the quality of a signal segment. The quality assessment can increase the accuracy of BR estimation using Kalman Filter (KF) or other algorithms, to reduce or eliminate the impact of low-quality segments on estimated BRs [14], [15]. This reduces the impact of noise, artifact or other disturbances. For example, the Signal Purity Index (SPI) uses Hjorth descriptors to assess signal quality by assuming that a perfect signal is a pure sinusoid [16]. The KF can be used to calculate a BR estimate from current and previous estimates weighted by their signal quality [4], [17]. The conventional KF assumes a linear model for the system dynamics, while most systems are nonlinear in nature. The linearization of the nonlinear model will be accompanied by errors, for which the Extended Kalman Filter (EKF) is used [18]. If BRs are obtained from multiple respiratory signals, then state vector fusion can be used to fuse the BRs to provide a single output. State vector fusion works based on the error covariance matrix [4].

In this paper, we propose an efficient algorithm to estimate BR, which employs promising methods in both time and frequency domains, while addressing their limitations. Multiple respiratory signals (EDRs, PDRs, or BDRs) are extracted from either an ECG, a PPG, or a BP signal using multiple methods (DWT and EMD methods). The respiratory signals are filtered using a KF, and then fused to produce a single respiratory signal. The BR is then estimated from this fused signal. The novelty of the proposed framework is that it creates a versatile structure that can use several methods for signal decomposition synchronously, evaluate the signal quality parameter to reduce the role of low quality parts of signal in estimation with help of EKF, and fuse the EDRs, PDRs, or BDRs to obtain a unique EDR, PDR, or BDR to estimate the BR. The paper is organized as follows. Section II describes the proposed algorithm, and the experimental methodology used to assess its performance. Section III presents the results, and the implications of these results are
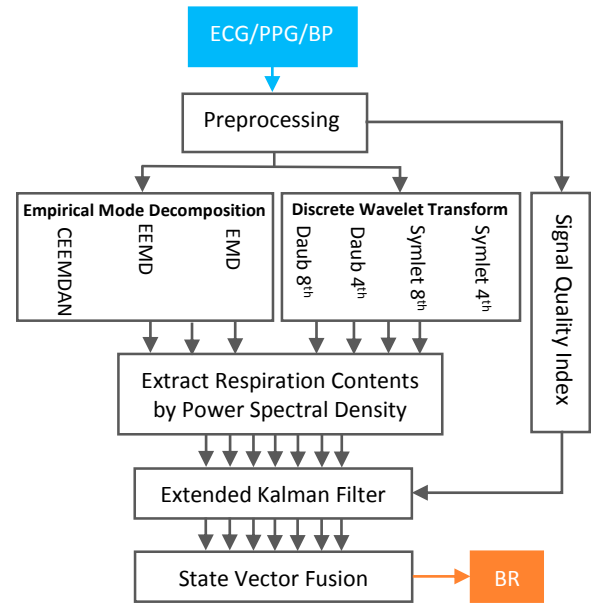

FIGURE 1. Block diagram of the proposed method, which estimates breathing rate (BR) from an electrocardiogram (ECG), a photoplethysmogram (PPG), or a blood pressure (BP) signal.

discussed in Section IV.

II. MATERIAL AND METHODS

A. PROPOSED ALGORITHM

The proposed algorithm is shown in Fig.1, and can be summarized as follows. Firstly, either an ECG, a PPG, or a BP signal is pre-processed to eliminate DC components and high-frequency noise. Secondly, DWT and EMD methods are used to decompose the signals into components. The PSDs of the components are used to identify components corresponding to respiratory signals (EDR, PDR, or BDR signals). Thirdly, the SPI is calculated over time for each respiratory signal, and is used with an EKF to remove the noise from each respiratory signal. The importance of the signal quality parameter in the EKF is more evident in the noisy parts which have low quality. Fourthly, state vector fusion is used to derive a single respiratory signal. Finally, the BR is estimated from the obtained respiratory signal using a peak detection algorithm.

1) Pre-Processing

A third-order Butterworth high-pass filter is applied to remove the DC component of the ECG, PPG, or BP signal. A cut-off frequency of $0.08 Hz$ was chosen for this filter based on the assumption that the lowest possible BR is 5 breaths per minute (bpm) ($0.083 Hz$). High-frequency noise is eliminated using a moving average filter with a window length of 11.
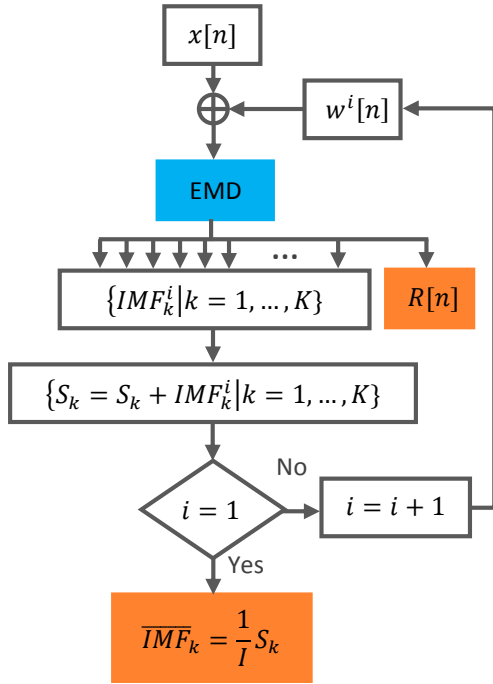
FIGURE 2. Flowchart of EEMD algorithm based on EMD algorithm.

FIGURE 3. Flowchart of CEEMDAN algorithm based on EEMD algorithm

2) Extracting Respiratory Signals

Two well-known methods with good decomposition performances were used to extract respiratory signals: EMD and its extended algorithm; and a DWT method. Each method was used to extract a set of respiratory signals from the input signal (either ECG, PPG, or BP). As demonstrated in Fig.1, three respiratory signals were extracted using the EMD method, and four were extracted using the DWT method. The EMD and DWT methods are now described.

i. Methods based on EMD

EMD is an adaptive fully data-driven method for analyzing non-linear and non-stationary signals [19]. By exploiting both local temporal and structural characteristics, time series are decomposed into individual components by expressing the original signal as a linear combination of zero-mean amplitude and frequency modulated functions called Intrinsic Mode Functions (IMFs), and a residual. Each IMF satisfies the following conditions: (1) the number of zero-crossings and positive/negative peaks should either be equal or at most differ by one; and (2) the mean of upper and lower envelopes must be zero [19].

The mode mixing problem arises when the signal contains intermittent processes. Mode mixing is defined as a single IMF containing signals of widely disparate scales or a signal of a similar scale residing in different components. This phenomenon makes the physiological meaning of individual IMFs unclear. To alleviate this problem a Noise-Assisted Data Analysis (NADA) method is proposed.
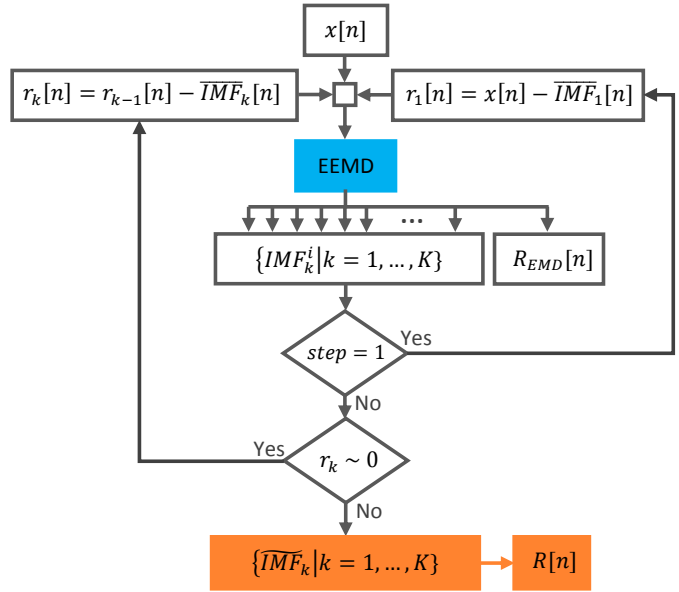
The Ensemble Empirical Mode Decomposition (EEMD) is based on the fact that the white noise could provide a uniformly distributed scale in time-frequency space. The EEMD method adds white noise to the signal to cause the components of a signal of different scales to automatically project onto proper scales of reference established by the white noise in the background [20].

The Complete Ensemble Empirical Mode Decomposition with Adaptive Noise (CEEMDAN), has been proven to be an important improvement on EEMD. The advantages of CEEMDAN over EEMD are that it achieves a negligible reconstruction error and solves the problem of different number of modes for different realizations of signal plus noise. EEMD and CEEMDAN methods are described further in [20]. The steps of the EEMD and CEEMDAN methods, are shown in the two flowcharts in Figs.2 and 3, respectively.

To determine which IMFs contain respiratory content, the PSD of each IMF is calculated, and the dominant frequency band of each IMF is identified as the $6dB$ bandwidth around the highest amplitude of the PSD. Afterwards, the IMF with the closest frequency band to the respiratory frequency band (6 to 33 bpm $[0.10Hz, 0.55Hz]$) is chosen as the EDR, PDR, or BDR signal.

Figs.4 and 5 show EDR and PDR signals extracted from a 60-second window of ECG and PPG signals respectively (from BIDMC01). These were extracted using EMD, EEMD and CEEMDAN methods. The dashed red and green lines indicate the dominant frequency ranges of the reference respiratory signal and EDR/PDR signals, respectively. The dominant frequency bands of both extracted EDR and PDR signals by CEEMDAN method are the closest to the dominant frequency band of the reference respiratory signal.
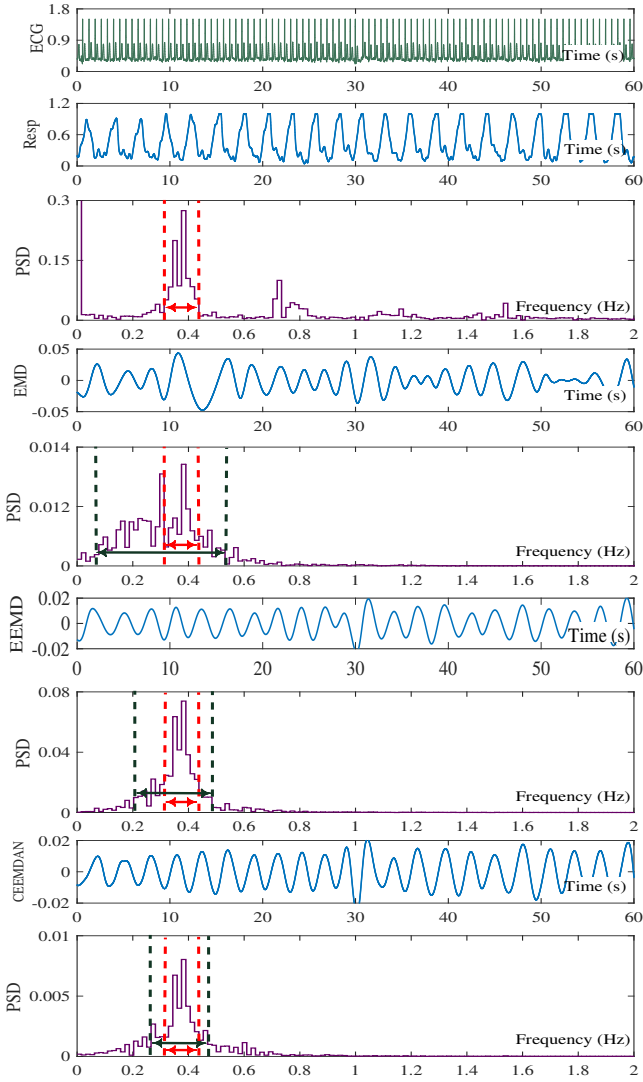
FIGURE 4. The ECG and the reference respiratory signals of subject BIDMC01 with extracted EDR signals by EMD, EEMD and CEEMDAN methods. The PSDs of the reference respiratory and EDR signals are shown under their corresponding signals. Red and green dotted lines specify the frequency bands of reference and derived respiratory signals, respectively.

FIGURE 5. The PPG and the reference respiratory signals of subject BIDMC01 with extracted PDR signals by EMD, EEMD and CEEMDAN methods. The PSDs of the reference respiratory and PDR signals are shown under their corresponding signals. Red and green dotted lines specify the frequency bands of reference and derived respiratory signals, respectively.

ii. Discrete Wavelet Transform:

The Wavelet Transform (WT) is a time-frequency signal analysis methods that offers simultaneous interpretation of the signal in both time and frequency domains, allowing local transient or intermittent components to be elucidated [21]. The WT and inverse transform can be computed discretely, quickly and without loss of signal information by considering the multiresolution algorithm. In this study, respiratory components of ECG, PPG, or BP signals were extracted using the DWT with four different mother wavelet functions: Daubechies of 4_{th} and 8_{th} order and Symlet of 4_{th} and 8_{th} order [22], [23]. After applying the DWT with these wavelet functions, the PSDs of each detail signal were calculated. To identify the detail signal containing respiratory content, the dominant frequency bands of the obtained PSDs were compared to the frequency band of respiration

$([0.10 Hz, 0.55 Hz])$.

Figs.6 and 7 show EDR and PDR signals extracted from 60 second windows of ECG and PPG signals (from BIDMC01) by applying the DWT with four different wavelet functions. As can be seen in Fig.6, the EDRs obtained by Symlet and Daubechies 8_{th} have the closest dominant frequency band to the dominant frequency range of the reference respiratory signal. This indicates their better performance than Symlet and Daubechies 4_{th}. The performance details of both mentioned wavelet functions with 4_{th} and 8_{th} orders are shown in the Results section as well. According to Fig.7, the dominant frequency bands of obtained PDRs for all four mentioned mother wavelets are not very different and their performance is lower than EDRs.
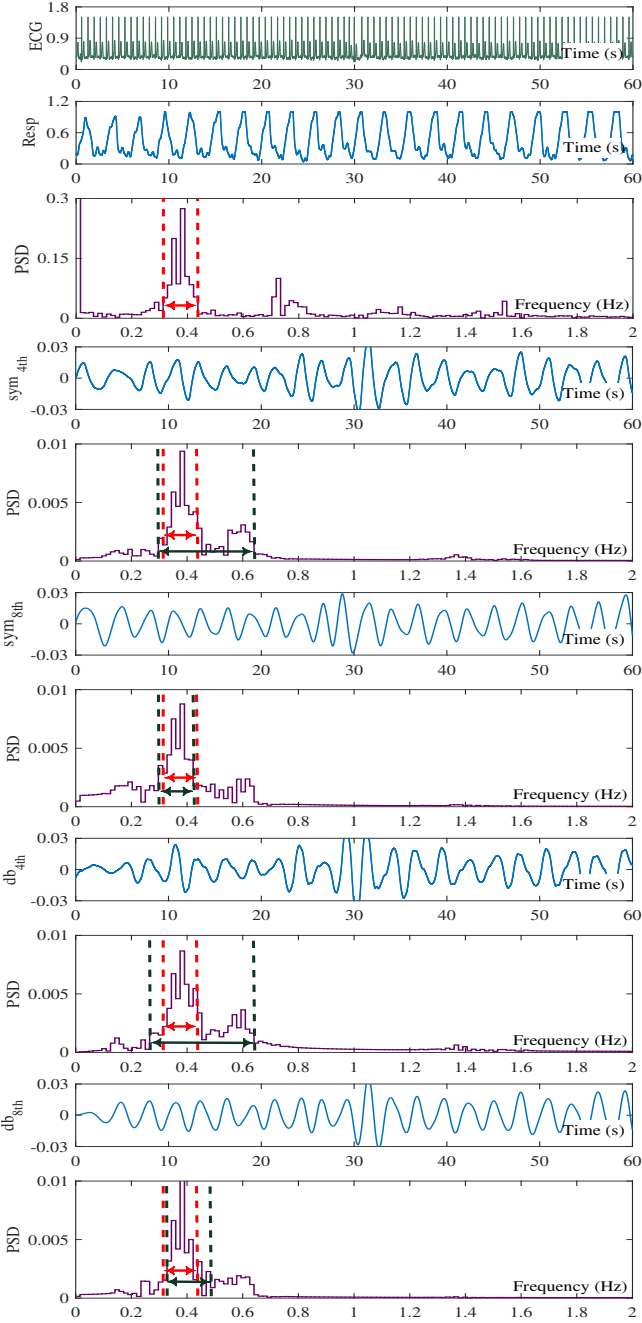
FIGURE 6. The ECG and the reference respiratory signals of subject BIDMC01 with extracted EDR signals using DWT mehtod. The PSDs of the reference respiratory and EDR signals are shown under their corresponding signals. Red and green dotted lines specify the frequency bands of reference and derived respiratory signals, respectively.
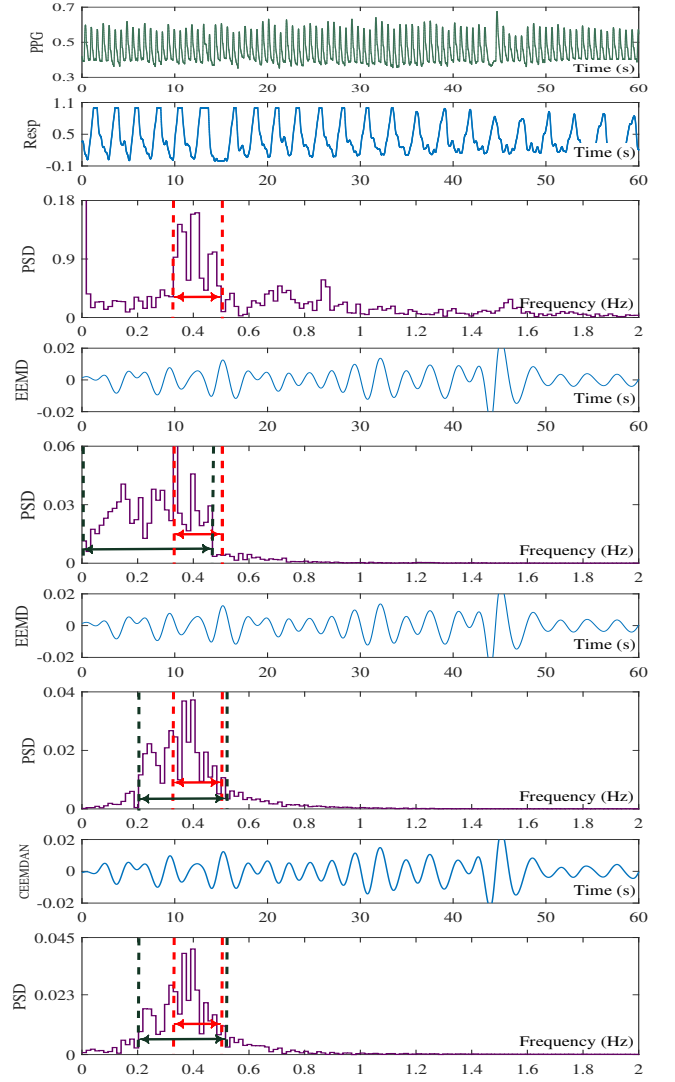
FIGURE 7. The PPG and the reference respiratory signals of subject BIDMC01 with extracted EDR signals using DWT method. The PSDs of the reference respiratory and PDR signals are shown under their corresponding signals. Red and green dotted lines respectively, specify the frequency bands of reference and derived respiratory signals.

3) Signal Quality Assessment

Hjorth parameters were originally proposed to extract features from the spectrum of the Electroencephalographic (EEG) signal by calculating moments of the EEG signal power spectrum [24]. The nth order spectral moment of a signal, $\overline{w}_n$, is defined as [16]:

$$\overline{w}_n = \int_{-\pi}^{\pi} w^n P(e^{j\omega}) d\omega \tag{1}$$

where $P(e^{j\omega})$ is the power spectrum of the signal as a function of angular frequency $\omega = 2\pi f$, with f in $cycles/second$. By averaging in the time domain, the spectral moments of a signal can be estimated using a shifting overlapping window as follows [16]:

$$\widetilde{\overline{w}}_i \approx \frac{2\pi}{L} \sum_{k=n-(L-1)}^{n} \left(x^{(\frac{i}{2})}(k) \right)^2 , \tag{2}$$
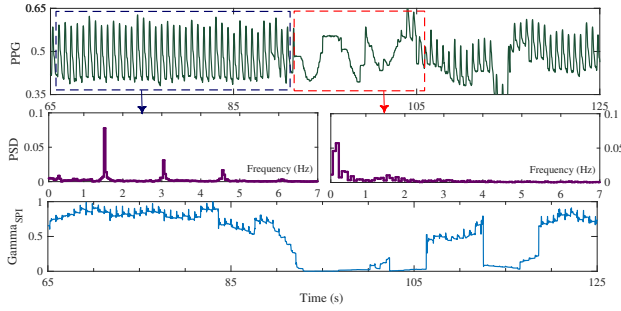
FIGURE 8. A 60-second window of PPG signal from subject BIDMC01 (top), along with the computed Γ_{SPI} (bottom). The power spectral densities (PSDs) of high and low quality parts of signal (marked with blue and red dotted rectangles, respectively) show the direct impact of signal PSD on Γ_{SPI} (middle).

where $x^{(\frac{i}{2})}(k)$ is the $i/2$ derivative of $x(k)$ and L is the window duration ($L = 4$s here). The SPI uses the Hjorth descriptors to calculate an index for assessing the quality of signals [16]. Here we have used SPI as an SQI to assess the quality of signals as follows:

$$\Gamma_{SPI}(n) = \frac{\overline{w}_2(n)^2}{\overline{w}_0(n)\overline{w}_4(n)} \quad . \tag{3}$$

Γ_{SPI} varies between 0 (corresponding to complete noise) and 1 (corresponding to a pure sinusoid), indicating low and high signal quality respectively. For instance, Fig.8 shows the variation of Γ_{SPI} for the PPG signal of BIDMC01, which approaches 0 during low quality periods and 1 during high quality periods.

4) Extended Kalman Filter

At this stage of the proposed algorithm, there are 7 respiratory signals, each with an accompanying SQI parameter. In this stage, the quality of the respiratory signals is improved by applying either a KF or EKF to them. Both a KF and an EKF can de-noise a signal and reconstruct the signal using a dynamic model. However, an EKF is able to accept a nonlinear dynamic model, whereas a KF is only able to accept a linear model. The process of linearizing a model for use with a KF can reduce its accuracy and consequently an EKF can provide better performance than a KF. In this work, the SQI parameter is used to optimize the EKF. Details are now provided on the use of the KF and EKF.

The KF is a well-known optimal state estimation method that has been proven to be the optimal filter in the Minimum Mean Square Error (MMSE) sense [25]. In practice, most systems exhibit non-linearity, and to apply the KF to nonlinear systems, the dynamical model must be first approximated to linear form, reducing the estimation accuracy. The EKF is an extension of the normal KF which considers nonlinear dynamic estimation of the states of a stochastic signal. The dynamic equations used as the state model in this paper are proposed by McSharry *et al* [26]. The dynamic model consists of three coupled ordinary differential equations. The details of the EKF can be found in [18].

At the time propagation stage, the EKF estimates the state vector by using the original nonlinear dynamical model of the signal. To estimate the state vector in each iteration, the EKF makes an interaction between dynamical model and measurements, which is created by Kalman Gain (KG). KG has an inverse relation with the value of the measurement noise covariance (R). Therefore, low quality measurements, which have higher R values, consequently have lower KG values. Decreasing the value of KG for each iteration reduces the effect of measurements in estimation and vice versa. A modification of R by a multiplicative factor is represented as [17]:

$$R_n \rightarrow R_n e^{(SQI_n{}^{-2}-1)} \tag{4}$$

where SQI_n is the SQI of the nth sample of data which is replaced by SPI in this paper, as follows:

$$SQI_n = \Gamma_{SPI}[n] \tag{5}$$

For low-quality parts of the signal, the value of $\Gamma_{SPI}[n]$ tends to zero. As a result, the value of R_n tends to infinity, and KG approaches zero. This indicates that the estimation for the low-quality parts of the signal is performed based on the dynamical model. This feature of the EKF enables us to have an acceptable estimation even for parts of the signal which are significantly distorted.

5) State Vector Fusion

At this stage of the proposed algorithm, there are 7 respiratory signals. State vector fusion is then used to fuse the 7 signals to provide a single respiratory signal. By considering the state error covariance matrices that are achieved from EKF, local estimate signals are combined in a MMSE sense [27], as follows:

$$\hat{x}_n = \left(\sum_{j=1}^{J} (P_n^j)^{-1}\right)^{-1} \sum_{j=1}^{J} [(P_n^j)^{-1} \hat{x}_n^j] \tag{6}$$

where $\hat{x}_n$ is the global estimate of state at each time n. J represents the number of signals that must be fused, which in our case is equal to 7 ($J = 7$). The $(P_n^j)^{-1}$ and $\hat{x}_n^j$, respectively are the inverses of the state error covariance matrices and the local state vector estimate for each of the 7 respiratory signals. According to this, respiratory signals with better performance contribute more to obtaining the state vector. In accordance to (6), for each sample of the 7 respiratory signals a global estimate of state is obtained as a single fused signal.

6) Estimating Breathing Rates

The method presented in [28] was used to detect the peaks in the fused respiratory signal. The BR was then estimated by counting the number of peaks within a time period, and expressed as beats per minute (*bpm*).

B. DATABASES

Two publicly available databases were used to assess the proposed algorithm when applied separately to ECG, PPG, and BP signals. Each database contains real-world physiological signals acquired during routine clinical practice. The databases contain real-world noise, including motion artifact, and periods of missing data. They also contain a range of BRs, ensuring that the signals used in this study are representative of those acquired in routine practice (the BR for each subject is provided in Tables VI and VII in the Appendix).

The first database was the MIT-BIH Polysomnographic Database [30], [31]. It contains 16 recordings from male subjects undergoing polysomnography (sleep assessment). Each recording is between 2 and 7 hours in duration and contains several physiological signals including the ECG, BP, and reference respiratory signals (mostly obtained using a nasal thermistor), which are sampled at 250Hz.

The second database was the BIDMC Database [31], [32]. It contains 53 recordings from critically-ill patients at the Beth Israel Deaconess Medical Centre (Boston, MA, USA). Each recording has a duration of 8 minutes, and contains several physiological signals including the ECG, PPG, and thoracic impedance (reference) respiratory signal, which are sampled at $125Hz$. The short recordings in this database were extracted from longer recordings in the MIMIC II Database, which were acquired during routine clinical practice.

Reference BRs for both databases were calculated by using a peak detection method to identify individual breaths in the reference respiratory signals.

C. COMPARISON OF ALGORITHMS

The proposed framework was applied to 60-second windows of ECG, PPG, and BP signals from each dataset. Its performance was compared to the following additional algorithms (which were each used firstly with an ECG as the input, secondly with a PPG as the input, and finally with a BP signal as the input):

- KF: the method summarised in Fig.1 but without including the SQI parameter and its effect on KF,
- EKF: the method summarised in Fig.1 but without including the SQI parameter and its effect on EKF,
- Smart Fusion Algorithm (SFA) [3],
- Autoregressive (AR) analysis [33],
- Principle Component Analysis (PCA) [34], and
- Kernel Principle Component Analysis (kPCA) [35].

D. ADDITION OF NOISE

The robustness of the proposed framework to noise was assessed by adding different levels of white noise to the input ECG, PPG, and BP signals and repeating the BR estimation. Five levels of noise were added to generate signals with a signal-to-noise ratio (SNR) of $SNR_{dB} = \{0, 5, 10, 20, 40\}$,

where

$$SNR_{dB} = 10\log_{10}\frac{\sum_{n=1}^{N}x[n]^2}{\sum_{n=1}^{N}(y[n]-x[n])^2} \quad (7)$$

where x is the original signal, y is the denoised signal and N is the total number of samples.

E. STATISTICAL ANALYSIS

The performance of BR algorithms was assessed by calculating three metrics.

- The Coverage Probability CP_δ: is the proportion of errors which fall within pre-defined bounds, δ. In this work an acceptable absolute error was defined as <2bpm. The non-parametric form of CP, expressed as a percentage, was calculated using the empirical cumulative distribution of the absolute error [36] with δ set at 2 bpm [6].
- The Mean Absolute Error (MAE):

$$\text{MAE} = \frac{1}{N}\sum_{i=1}^{N}|\hat{\mu}_{BR}(i) - \mu_{ref}(i)|, (bpm) \quad (8)$$

where $\hat{\mu}_{BR}(i)$ and $\mu_{ref}(i)$ represent the estimated BR and reference BR, respectively, and N is the number of windows over the entire database [37].
- The Mean Absolute Percentage Error (MAPE):

$$\text{MAPE} = \frac{1}{N}\sum_{i=1}^{N}|\frac{\hat{\mu}_{BR}(i) - \mu_{ref}(i)}{\mu_{ref}(i)}| \times 100, (\%) \quad (9)$$

The quality of each subject's ECG, PPG, or BP signals was assessed using a parameter called Q, which is the percentage ratio of the number of low quality windows N_l to the total number of windows N_T of each signal:

$$Q = \frac{N_l}{N_T} \times 100\% \quad . \quad (10)$$

Windows were deemed to be of low quality if the average of Γ_{SPI} in that window was lower than 0.5.

Throughout the analysis windows of 60 seconds duration with 50% overlap were used.

III. RESULTS

A. COMPARISON OF CEEMDAN AND DWT METHODS

In this section, we compare the performances of the DWT and CEEMDAN methods for estimating BR, considering overall performances, and performances across different BR ranges. Table I shows the MAPE for CEEMDAN and DWT ($db8_{th}$) methods for ECG, PPG and BP signals in each dataset. According to Table I, the CEEMDAN method performed better than DWT method at lower BRs $< 16bpm$, with the exception of PPG data from the BIDMC database. At higher BRs $> 16bpm$, the DWT method performed better.

Fig.9 shows a comparison of the performances of CEEMDAN and DWT methods across different BR ranges. For BRs lower than $16bpm$, the CEEMDAN method performed best, and for BRs higher than $16bpm$, the DWT method performed

TABLE I. The performance of CEEMDAN and DWT ($db8_{th}$) BR estimation algorithms, expressed in MAPE.

Reference BR	BIDMC		MIT-BIH	
	CEEMDAN	DWT	CEEMDAN	DWT
ECG signals				
$< 12bpm$	6.7	7.3	6.2	6.6
$12 - 16bpm$	4.3	4.5	3.9	4.3
$16 - 20bpm$	4.9	3.6	4.7	3.4
$> 20bpm$	4.5	2.9	4.2	3.1
Entire database	4.8	4.1	4.6	3.9
PPG signals			*BP signals*	
$< 12bpm$	8.7	7.5	6.9	7.3
$12 - 16bpm$	7.5	6.6	5.0	5.3
$16 - 20bpm$	5.9	4.8	4.9	4.6
$> 20bpm$	5.1	3.6	4.4	3.5
Entire database	6.5	5.4	5.0	4.8

FIGURE 9. The performance of CEEMDAN and DWT methods for estimating BR from ECG, PPG, and BP signals (expressed as MAPE). These results obtained from both of MIT-BIH Polysomnographic and BIDMC databases.

TABLE II. Overall performance summary of methods applied to ECG*, PPG and BP signals of the MIT-BIH Polysomnographic and BIDMC databases.

Algorithm	ECG signals			PPG signals			BP signals		
	CP_2 (%)	MAE (bpm)	MAPE (%)	CP_2 (%)	MAE (bpm)	MAPE (%)	CP_2 (%)	MAE (bpm)	MAPE (%)
SFA	63.7	1.15	6.4	57.1	1.26	6.9	54.8	1.33	7.3
AR	60.8	1.24	6.9	58.0	1.20	6.7	53.4	1.31	7.1
PCA	54.6	1.15	6.4	53.2	1.27	7.0	49.2	1.30	7.4
kPCA	69.7	1.06	5.9	63.0	1.16	6.5	59.9	1.17	6.5
EMD	58.9	1.19	6.6	55.1	1.28	7.0	50.4	1.33	7.8
EEMD	67.2	0.95	5.3	65.2	1.09	5.7	58.7	1.24	7.2
CEEMDAN	70.9	0.95	5.3	67.8	1.09	6.0	60.1	1.01	5.8
DWT($sym4_{th}$)	70.5	1.15	6.4	65.9	1.12	6.9	66.2	1.07	6.8
DWT($db4_{th}$)	66.1	1.13	6.3	60.1	1.20	6.9	51.9	1.35	7.4
DWT($sym8_{th}$)	69.8	0.90	5.0	66.0	1.14	6.4	57.1	1.25	7.3
DWT($db8_{th}$)	71.3	0.92	5.1	68.3	1.05	5.6	61.8	1.23	6.7
KF	79.6	0.88	4.9	68.2	0.95	5.3	63.7	1.20	6.7
EKF	82.0	0.76	4.2	72.1	0.81	4.9	70.8	1.00	5.4
Our Framework	87.8	0.63	3.5	79.8	0.73	4.1	81.2	0.69	4.0

*The average of obtained results from ECG records of the MIT-BIH Polysomnographic and BIDMC databases.

with low quality signals (see Table VII for details).

As noted in Table VII, BRs could not be estimated from subject BIDMC32's ECG due to the lack of respiratory content in this signal.

Table II shows the overall performances of methods for the ECG, PPG and BP signals on the BIDMC and MIT-BIH databases, assessed using CP_2, MAE, and MAPE.

C. THE IMPACT OF NOISE

The proposed framework's robustness to noise was assessed in two steps. Firstly, performance was assessed with and without the framework's SQI parameter. Secondly, performance was assessed in the presence of different levels of added noise. In order to evaluate the proposed method, different portions of white Gaussian noises have been added to ECG, PPG, and BP signals from BIDMC and MIT-BIH databases. The results for ECG, PPG, and BP signals are shown in Tables III, IV, and V, respectively.

BRs were estimated using the proposed framework with and without the SQI parameter (described in Section II-A3) in order to assess the importance of the signal quality assessment step. According to the results in Tables III and IV, PCA and kPCA algorithms performed better than AR and SFA methods at a low level of noise. However, the PCA and kPCA algorithms were very sensitive to noise and their performance declined at higher noise levels. AR analysis (a frequency domain method) was more robust against additive noise.

A comparison of results obtained using EKF (without the SQI) and our proposed framework can further explain the role of the SQI in improving performance. For example, for the BR range of $16 - 20bpm$ with $SNR = 40dB$ (Table.IV), our framework showed 0.8% improvement compared to EKF. Changing the SNR value from 40 to 0 dB, the average MAPE increased less for our framework ($6.4\% - 4.2\% = 2.2\%$ increase) than for EKF ($7.7\% - 5.0\% = 2.7\%$). This shows that the SQI parameter increased the algorithm's robustness to noise.

In the following, the advantage of the CEEMDAN method over EMD and EEMD methods in accuracy and robustness

best. This suggests that neither method is superior to the other. A comparison of performance between ECG, PPG, and BP signals shows the best results are obtained from ECG signals, although the differences are not substantial. The PPG signal is often easier to obtain than ECG and BP signals, so may still be advantageous in several settings.

B. THE PERFORMANCE OF THE PROPOSED FRAMEWORK

The average MAPEs of BR estimation on the MIT-BIH Polysomnographic and BIDMC databases were 3.9% and 3.6% for ECG signals, 6.0% for PPG, and 5.0% for BP signals (patient-level data are provided in Tables VI and VII in the Appendix). The proposed framework for estimating BR performed well even in the presence of a high volume of the noise and artifacts. For instance, subject BIDMC40 had a Q_{PPG} value of 74.3%, indicating that their signals were generally of low quality, yet a MAPE of only 11.8%, demonstrating the ability of the method to perform well even
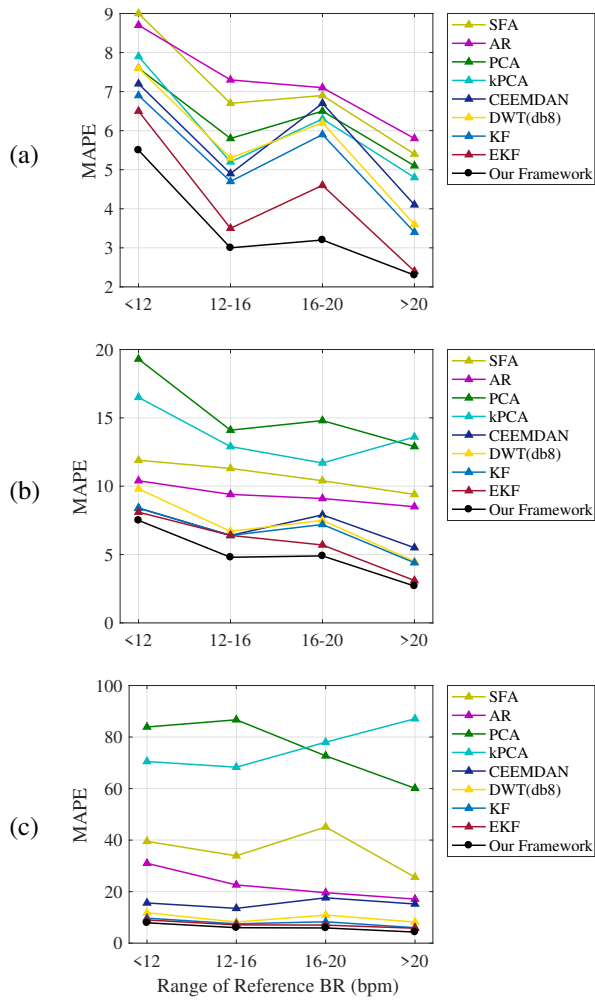
FIGURE 10. The performance of methods applied to ECG signals of the MIT-BIH Polysomnographic and BIDMC databases in the presence of added noise, expressed as MAPE. (a) $SNR = 40dB$, (b) $SNR = 10dB$, (c) $SNR = 0dB$.

FIGURE 11. The performance of methods applied to BP signals of the MIT-BIH Polysomnographic database in the presence of added noise, expressed as MAPE. (a) $SNR = 40dB$, (b) $SNR = 10dB$, (c) $SNR = 0dB$.

can be observed. In Table III the changes in MAPE for EMD and CEEMDN methods in the range of $12-16$ bpm are (from SNR=$40dB$ to SNR=$0dB$), 12.2% ($18.9\% - 6.7\%$) and 8.6% ($13.5\% - 4.9\%$) respectively (which are similar to those of other BR ranges). The performance of the DWT method is close to that of the CEEMDAN method but the results show that CEEMDAN is more robust to additive noise than DWT.

The improvement in performance when using a fusion method (either EKF or our framework) compared to using a single respiratory signal (EMD, EEMD, CEEMDAN or DWT) demonstrates the importance of the fusion part of the algorithm. The EKF and state vector fusion in our algorithm resulted in significant reduction in MAPE.

Comparison of the performance of the mentioned methods is illustrated in Figs.10 and 11. Fig.10 represents the results which have been obtained from ECG signals and Fig.11 shows the results for BP signals. The KF method showed a poorer performance than EKF method which can be explained by the impact of approximation for linearization of the nonlinear signal model. On the other hand, the performance difference between KF and EKF is due to the linear and nonlinear consideration of the model. In estimating the BR from a respiratory signal, the effect of detecting a false peak is lower for higher reference BRs. This may explain the general trend of lower MAPEs at higher BRs in Fig.10 and 11. According to these two figures, our framework has shown the best performance and highest resistance to noise than other methods.

IV. DISCUSSION AND CONCLUSION

In this study we proposed a framework to estimate BR from ECG, PPG, or BP signals. The performance of the framework was assessed on two publicly available datasets, and compared to that of previously proposed methods. The results indicate that our proposed framework shows high accuracy, and good robustness even in presence of noise.

Our framework uses both EMD and DWT methods to extract respiratory signals, obtain the advantages of each. This study did not investigate which had better performance

TABLE III. Overall performance summary of methods applied to ECG* signals of the MIT-BIH Polysomnographic and BIDMC databases in the presence of added noise, expressed as MAPE.

Algorithm	$< 12bpm$					$12 - 16bpm$					$16 - 20bpm$					$> 20bpm$				
	$SNR = 40, 20, 10, 5, 0(dB)$					$SNR = 40, 20, 10, 5, 0(dB)$					$SNR = 40, 20, 10, 5, 0(dB)$					$SNR = 40, 20, 10, 5, 0(dB)$				
SFA	9	9.8	11.9	22.8	39.5	6.7	7.9	11.3	17.5	33.9	6.9	7.8	10.4	19.0	45.1	5.4	6.6	9.4	12.7	25.6
AR	8.7	9.1	10.4	16.4	31.0	7.3	7.8	9.4	15.0	22.6	6.1	7.5	9.1	13.9	19.6	5.8	6.1	8.5	10.8	15.5
PCA	7.6	10.8	19.3	47.1	83.9	5.8	9.1	14.1	34.8	86.7	6.5	10.2	14.8	37.1	72.7	5.1	8.6	12.9	32.5	60.1
kPCA	7.9	10.6	16.5	29.6	70.5	5.2	8.1	12.9	31.5	68.3	6.3	7.9	11.7	23.9	78.0	4.8	7.6	13.6	34.9	87.1
EMD	9.3	9.9	11.2	18.9	27.8	6.7	7.4	8.6	12.7	18.9	7.3	9.1	9.4	16.6	21.3	5.4	5.9	7.2	10.9	17.2
EEMD	7.2	8.3	10.6	16.0	19.5	5.7	6.0	7.1	12.4	16.2	6.9	7.3	8.8	13.7	19.1	4.9	5.3	6.1	11.0	16.3
CEEMDAN	7.2	7.5	8.4	10.8	15.6	4.9	5.3	6.4	9.8	13.5	6.7	7.1	7.9	11.4	17.6	4.1	4.6	5.5	7.8	15.2
DWT (sym4$_{th}$)	9.2	9.7	10.5	12.6	14.1	6.4	6.9	8.5	10.1	15.7	6.4	7.4	9.0	10.3	13.9	5.7	6.5	7.8	11.6	14.1
DWT (db4$_{th}$)	8.3	9.9	11.0	12.3	15.6	6.7	7.3	8.9	10.8	14.9	6.5	7.9	10.2	12.5	14.7	5.4	6.1	7.6	10.7	13.9
DWT (sym8$_{th}$)	7.5	8.1	9.3	10.1	12.9	5.4	6.1	6.9	7.8	9.3	5.9	6.7	7.9	9.3	12.6	4.1	4.8	5.6	6.1	9.7
DWT (db8$_{th}$)	7.6	8.4	9.8	10.5	11.8	5.3	5.6	6.7	6.9	8.2	6.2	6.7	7.5	8.1	10.9	3.6	3.8	4.5	5.7	8.2
KF	6.9	7.4	8.4	9.1	9.7	4.7	5.2	6.4	6.9	7.5	5.9	6.5	7.2	7.9	8.3	3.4	3.3	4.4	4.9	6.0
EKF	6.5	7.3	8.1	8.3	9.0	3.5	5.0	6.4	6.8	7.1	4.6	5.2	5.7	7.0	7.0	2.4	2.6	3.1	4.0	5.8
Our Framework	**5.5**	**6.2**	**7.5**	**7.8**	**7.9**	**3.0**	**3.8**	**4.8**	**5.4**	**6.0**	**3.2**	**3.7**	**4.9**	**5.1**	**5.9**	**2.3**	**2.3**	**2.7**	**3.1**	**4.3**
Average	7.8	8.8	10.9	16.6	26.3	5.7	6.6	8.6	13.5	23.5	6.2	7.2	8.9	14.0	24.8	4.5	5.3	7.1	12.3	21.5

*The average of obtained results from ECG records of MIT-BIH Polysomnographic and BIDMC databases.

TABLE IV. Overall performance summary of methods applied to PPG signals of the BIDMC database in the presence of added noise, expressed as MAPE.

Algorithm	$< 12bpm$					$12 - 16bpm$					$16 - 20bpm$					$> 20bpm$				
	$SNR = 40, 20, 10, 5, 0(dB)$					$SNR = 40, 20, 10, 5, 0(dB)$					$SNR = 40, 20, 10, 5, 0(dB)$					$SNR = 40, 20, 10, 5, 0(dB)$				
SFA	8.1	9.3	9.8	15.6	27.9	7.5	8.1	10.3	19.2	33.4	6.4	6.9	9.0	16.7	29.1	6.8	7.9	10.1	19.2	34.5
AR	9.0	9.9	11.0	14.2	24.8	6.8	7.9	9.2	15.4	23.7	6.5	7.3	8.7	13.9	25.8	6.3	7.2	9.6	14.3	22.8
PCA	7.3	9.8	15.4	29.8	65.4	7.1	8.7	14.7	25.5	48.2	6.5	8.6	19.1	37.8	74.5	5.2	7.4	13.7	35.6	73.1
kPCA	7.5	9.0	13.9	27.5	59.6	6.7	9.3	15.0	24.7	67.8	6.1	9.2	15.4	30.3	64.9	5.4	7.1	10.2	17.9	62.9
EMD	8.9	9.3	11.0	13.9	21.6	7.4	8.2	10.1	13.5	23.7	7.9	8.4	10.3	15.9	22.9	6.7	7.0	8.3	14.7	22.3
EEMD	7.5	8.1	9.9	11.9	14.7	6.2	7.4	9.3	12.0	19.0	6.4	6.9	7.5	10.9	18.4	4.8	5.4	7.0	8.8	14.9
CEEMDAN	7.6	7.7	8.9	12.0	14.5	4.3	4.5	5.4	9.9	13.8	6.1	6.5	7.8	11.9	17.8	4.1	4.7	6.4	10.5	22.6
DWT (sym4$_{th}$)	8.3	9.8	11.6	13.8	16.9	6.7	7.1	8.0	10.6	13.2	7.5	7.9	8.4	9.7	14.7	4.9	5.4	6.7	10.1	21.7
DWT (db4$_{th}$)	8.2	9.5	12.5	14.7	18.4	7.6	7.9	8.5	12.8	21.6	6.9	7.5	8.0	12.1	17.8	6.1	6.6	8.1	12.4	18.4
DWT (sym8$_{th}$)	7.5	8.6	10.9	12.0	15.5	6.4	6.5	7.4	8.8	13.4	5.7	6.2	7.3	9.0	12.8	4.2	4.5	6.1	8.2	11.3
DWT (db8$_{th}$)	7.7	8.3	11.3	13.4	18.2	5.6	6.0	6.9	8.7	11.9	5.5	5.8	6.8	7.5	10.9	4.1	4.3	5.2	5.9	7.9
KF	7.4	7.5	8.9	9.3	10.2	4.1	4.3	5.3	6.2	7.9	5.0	5.7	6.6	7.0	8.5	3.7	4.2	4.9	5.8	6.9
EKF	6.6	7.0	8.3	9.0	9.7	3.6	4.4	5.2	6.9	7.7	5.0	5.3	5.9	6.7	7.7	3.7	4.0	4.8	5.3	6.9
Our Framework	**6.2**	**6.6**	**7.2**	**8.2**	**9.3**	**3.5**	**4.2**	**5.3**	**6.3**	**7.3**	**4.2**	**4.6**	**5.1**	**5.7**	**6.4**	**3.2**	**3.5**	**4.1**	**4.5**	**5.4**
Average	7.7	8.6	10.8	14.7	23.3	6.0	6.8	8.6	13.0	22.3	6.1	6.9	9.0	13.9	23.7	4.9	5.7	7.5	12.4	23.7

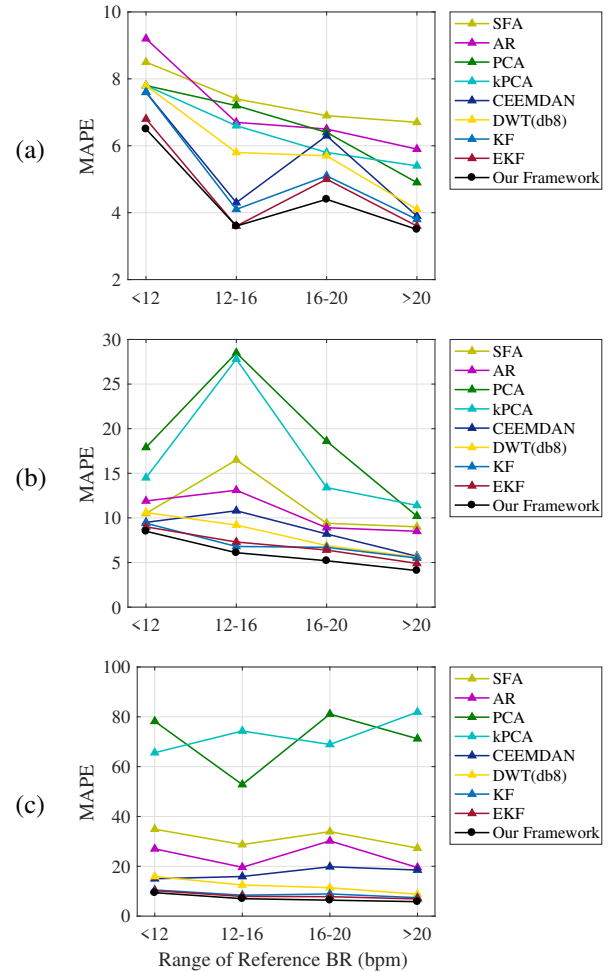**TABLE V.** Overall performance summary of methods applied to BP signals of the MIT-BIH Polysomnographic database in the presence of added noise, expressed as MAPE.

Algorithm	$< 12bpm$					$12 - 16bpm$					$16 - 20bpm$					$> 20bpm$				
	$SNR = 40, 20, 10, 5, 0(dB)$					$SNR = 40, 20, 10, 5, 0(dB)$					$SNR = 40, 20, 10, 5, 0(dB)$					$SNR = 40, 20, 10, 5, 0(dB)$				
SFA	8.9	9.7	11.2	18.8	41.9	7.3	8.1	9.1	13.8	24.0	7.4	8.5	9.8	19.7	38.7	6.6	6.9	7.9	12.0	20.1
AR	9.4	10.9	12.8	17.0	29.2	6.6	7.5	7.9	10.8	15.5	6.5	7.5	9.1	16.9	34.6	5.5	6.4	7.4	10.5	16.2
PCA	8.3	11.2	20.4	38.4	91.0	7.3	9.9	18.1	31.5	57.4	6.3	7.6	18.1	36.0	87.7	4.6	6.0	6.7	25.2	69.3
kPCA	8.1	9.2	15.1	34.1	71.6	6.5	8.5	12.8	30.9	80.0	5.5	8.2	11.4	33.3	72.9	5.4	7.3	12.6	21.1	77.9
EMD	9.5	9.9	12.4	16.7	27.8	8.4	9.4	11.5	16.9	24.3	8.9	9.8	11.9	19.3	26.7	6.3	6.6	7.5	10.3	14.3
EEMD	8.3	9.5	11.5	13.9	18.9	6.4	7.4	8.5	11.0	16.6	7.0	7.3	8.3	12.1	22.4	4.8	5.8	7.4	9.4	18.3
CEEMDAN	7.6	8.5	10.1	13.4	15.5	4.3	4.5	5.8	11.7	18.0	6.5	7.3	8.6	15.3	21.8	3.7	4.1	5.0	7.9	14.4
DWT (sym4$_{th}$)	9.1	11.0	14.0	14.2	20.5	7.1	7.3	9.0	12.0	16.4	7.7	8.5	9.6	11.7	16.5	4.9	6.0	6.9	11.7	21.1
DWT (db4$_{th}$)	8.2	10.3	13.7	16.1	20.8.4	6.8	7.1	7.5	10.6	19.0	7.3	8.3	9.6	15.1	21.0	5.9	6.2	6.8	10.6	18.4
DWT (sym8$_{th}$)	8.3	9.2	12.5	15.6	17.5	6.4	6.5	8.2	9.2	11.8	5.3	5.6	6.1	8.0	10.2	3.8	3.9	5.5	7.0	8.3
DWT (db8$_{th}$)	7.9	8.5	9.9	10.0	13.6	6.0	6.2	7.5	9.7	13.1	5.9	6.0	7.0	8.1	11.9	4.1	4.5	6.0	6.5	9.7
KF	7.8	8.1	8.9	9.9	10.8	4.1	4.7	5.9	7.4	8.9	5.2	5.7	6.8	7.2	9.3	3.9	4.4	6.1	6.8	7.9
EKF	7.0	7.8	9.7	10.2	10.7	3.6	5.0	6.4	7.7	8.1	5.0	5.5	6.9	7.3	8.4	3.5	4.0	5.0	5.3	6.9
Our Framework	**6.8**	**7.8**	**8.2**	**8.9**	**9.5**	**3.7**	**4.2**	**5.3**	**5.9**	**6.7**	**4.6**	**4.8**	**5.3**	**5.9**	**6.4**	**3.3**	**3.7**	**4.1**	**4.9**	**6.2**
Average	8.2	9.4	12.4	17.0	28.5	6.1	6.9	8.8	13.5	22.5	6.4	7.2	9.2	15.4	27.7	4.8	5.4	6.7	10.6	22.6

for extracting EDR, PDR, and BDR signals, although the superior EMD and DWT methods (CEEMDAN and $db8_{th}$) gave broadly similar performance.

The EKF method, taking into account the dynamical model for the EDR, PDR, and BDR signals, gave the framework the ability to work well even in low quality parts of ECG, PPG, or BP signals. The inclusion of the SQI parameter in the EKF increased performance.

Finally, considering the method of state vector fusion in our framework, give this capability to our framework to increase the effect of better estimation on output, which results in a single output with high precision.

Some previously proposed methods showed lower robustness to additive noise, especially the methods of PCA and kPCA. This may be because these methods involve identifying fiducial points, such as QRS-complexes in ECG signals, or systolic peaks in PPG signals, which can be confounded by noise. Although SFA also involves identifying fiducial points, it showed better performance in presence of noise. The AR method was also less sensitive to noise, although it is based on the assumption of a relatively constant BR in each window of ECG, PPG, or BP signals.

In our new framework (summarised in Fig.1), we utilized time and frequency domain methods to increase the accuracy of BR estimation and also make the algorithm robust in presence of noise. The most important advantage of our framework is that it has a regular and stable structure which is able to estimate BR from ECG, PPG, or BP signals with different morphologies completely automatically. The structure is designed to select the best extracted EDR, PDR, or BDR signal, and estimate the BR based on that signal, which improves the performance of our proposed method. Furthermore, using the modified EKF with SQI, it can automatically recover parts of respiratory signals that have been distorted. Despite these advantages, the simultaneous use of several methods increases the complexity of the algorithm. Nevertheless, it could be advantageous in scenarios with greater levels of noise and artifact, such as during exercise. Further work is required to investigate whether it does indeed confer benefit in these scenarios.

In the future, we plan to test our proposed framework on stress data which will pose greater challenges. The performance of the framework should also be assessed in the presence of arrhythmias such as atrial fibrillation, and with very noisy signals, to determine whether it provides reliable BR estimates in such scenarios. In addition, the framework may have other applications to estimate parameters from physiological signals, such as measuring the depth of anesthesia from EEG signals. Future work should also consider assessing the performance of BR algorithms when run in real-time, considering the limited computational and memory specifications of wearable sensors.

REFERENCES

[1] R. M. Schein, N. Hazday, M. Pena, B. H. Ruben, and C. L. Sprung, "Clinical antecedents to in-hospital cardiopulmonary arrest," *Chest*, vol. 98, no. 6, pp. 1388-1392, 1990, doi: 10.1378/chest.98.6.1388.

[2] K. Mochizuki, R. Shintani, K. Mori, T. Sato, O. Sakaguchi, K. Takeshige, K. Nitta, and H. Imamura, "Importance of respiratory rate for the prediction of clinical deterioration after emergency department discharge: a single-center, case–control study," *Acute Med. Surg.*, vol. 4, no. 2, pp. 172-178, 2017, doi: 10.1002/ams2.252.

[3] W. Karlen, S. Raman, J. M. Ansermino, and G. A. Dumont, "Multiparameter respiratory rate estimation from the photoplethysmogram," *IEEE Trans. Biomed. Eng.*, vol. 60, no. 7, pp. 1946–1953, 2013, doi: 10.1109/TBME.2013.2246160.

[4] L. Mason, *Signal processing methods for non-invasive respiration monitoring*, University of Oxford, Oxford, UK, 2002, [Online]. Available: http://www.ibme.ox.ac.uk/research.

[5] M. A. Pimentel, P. H. Charlton, and D. A. Clifton, "Probabilistic estimation of respiratory rate from wearable sensors," *Wearable Electronics Sensors*. Springer, vol. 15, pp. 241–262, 2015, doi: 10.1007/978-3-319-18191-2_10.

[6] P. H. Charlton, T. Bonnici, L. Tarassenko, D. A. Clifton, R. Beale, and P. J. Watkinson, "An assessment of algorithms to estimate respiratory rate from the electrocardiogram and photoplethysmogram," *Physiol. Meas.*, vol. 37, no. 4, p. 610, 2016, doi: 10.1088/0967-3334/37/4/610.

[7] P. H. Charlton, D. A. Birrenkott, T. Bonnici, M. A. Pimentel, A. E. Johnson, J. Alastruey, L. Tarassenko, P. J. Watkinson, R. Beale, and D. A. Clifton, "Breathing rate estimation from the electrocardiogram and photoplethysmogram: A review," *IEEE Rev. Biomed. Eng.*, vol. 11, pp. 2–20, 2017, doi: 10.1109/RBME.2017.2763681.

[8] K. V. Madhav, M. R. Ram, E. H. Krishna, N. R. Komalla, and K. A. Reddy, "Estimation of respiration rate from ecg, bp and ppg signals using empirical mode decomposition," in *Proc. IEEE Conf. Int. Instrum. Meas. Technol.*. IEEE, 2011, pp. 1–4, doi: 10.1109/IMTC.2011.5944249.

[9] D. Labate, F. La Foresta, G. Occhiuto, F. C. Morabito, A. Lay-Ekuakille, and P. Vergallo, "Empirical mode decomposition vs. wavelet decomposition for the extraction of respiratory signal from single-channel ecg: A comparison," *IEEE Sensors J.*, vol. 13, no. 7, pp. 2666–2674, 2013, doi: 10.1109/JSEN.2013.2257742.

[10] Y. D. Lin and Y. F. Jhou, "Estimation of heart rate and respiratory rate from the seismocardiogram under resting state," *Biomed. Signal Process Control*, vol. 57, p. 101779, 2020, doi: 10.1016/j.bspc.2019.101779.

[11] O. M. Solomon Jr, "Psd computations using welch's method. [power spectral density (psd)]," Sandia National Labs., Albuquerque, NM (United States), Tech. Rep., 1991.

[12] R. Bailón, L. Sornmo, and P. Laguna, "A robust method for ecg-based estimation of the respiratory frequency during stress testing," *IEEE Trans. Biomed. Eng.*, vol. 53, no. 7, pp. 1273–1285, 2006, doi: 10.1109/TBME.2006.871888.

[13] J. Lázaro, E. Gil, R. Bailón, A. Mincholé, and P. Laguna, "Deriving respiration from photoplethysmographic pulse width," *Med. Biol. Eng. Comput.*, vol. 51, no. 1-2, pp. 233–242, 2013, doi: 10.1007/s11517-012-0954-0.

[14] G. D. Clifford, W. Long, G. Moody, and P. Szolovits, "Robust parameter extraction for decision support using multimodal intensive care data," *Philos. Trans. Royal Soc. A: Math., Phys. and Eng. Sci.*, vol. 367, no. 1887, pp. 411–429, 2009, doi: 10.1098/rsta.2008.0157.

[15] S. Nemati, A. Malhotra, and G. D. Clifford, "Data fusion for improved respiration rate estimation," *EURASIP J. Adv. Signal Process.*, vol. 2010, no. 1, p. 926305, 2010, doi: 10.1155/2010/926305.

[16] L. Sörnmo, and P. Laguna, *Bioelectrical signal processing in cardiac and neurological applications*. Academic Press, 2005, vol. 8.

[17] Q. Li, R. G. Mark, and G. D. Clifford, "Robust heart rate estimation from multiple asynchronous noisy sources using signal quality indices and a kalman filter," *Physiol. Meas.*, vol. 29, no. 1, p. 15, 2007, doi: 10.1088/0967-3334/29/1/002.

[18] R. Sameni, M. B. Shamsollahi, C. Jutten, and G. D. Clifford, "A nonlinear bayesian filtering framework for ecg denoising," *IEEE Trans. Biomed. Eng.*, vol. 54, no. 12, pp. 2172–2185, 2007, doi: 10.1109/TBME.2007.897817.

[19] N. E. Huang, Z. Shen, S. R. Long, M. C. Wu, H. H. Shih, Q. Zheng, N. C. Yen, C. C. Tung, and H. H. Liu, "The empirical mode decomposition and the hilbert spectrum for nonlinear and non-stationary time series analysis," *Proc. Royal Soc. London. Ser. A: Math. Phys. Eng. Sci.*, vol. 454, no. 1971, pp. 903–995, 1998, doi: 10.1098/rspa.1998.0193.

[20] M. E. Torres, M. A. Colominas, G. Schlotthauer, and P. Flandrin, "A complete ensemble empirical mode decomposition with adaptive noise,"

in *Proc. Int. Conf. Acoust., Speech Signal Process.* IEEE, 2011, pp. 4144–4147, doi: 10.1109/ICASSP.2011.5947265.

[21] S. Mallat and W. L. Hwang, "Singularity detection and processing with wavelets," *IEEE Trans. Inf. Theory*, vol. 38, no. 2, pp. 617–643, 1992, doi: 10.1109/18.119727.

[22] A. C. Rowe and P. C. Abbott, "Daubechies wavelets and mathematica," *Comput. Phys.*, vol. 9, no. 6, pp. 635–648, 1995, doi:10.1063/1.168556.

[23] G. Strang and T. Nguyen, *Wavelets and filter banks*. SIAM, 1996.

[24] B. Hjorth, "The physical significance of time domain descriptors in eeg analysis," *Electroencephalogr. Clin. Neurophysiol.*, vol. 34, no. 3, pp. 321–325, 1973, doi: 10.1016/0013-4694(73)90260-5.

[25] S. M. Kay, *Fundamentals of statistical signal processing*. Prentice-Hall, 1993.

[26] P. E. McSharry, G. D. Clifford, L. Tarassenko, and L. A. Smith, "A dynamical model for generating synthetic electrocardiogram signals," *IEEE Trans. Biomed. Eng.*, vol. 50, no. 3, pp. 289–294, 2003, doi: 10.1109/TBME.2003.808805.

[27] Q. Gan and C. J. Harris, "Comparison of two measurement fusion methods for kalman filter based multisensor data fusion," *IEEE Trans. Aerosp. Electron. Syst.*, vol. 37, no. 1, pp. 273–279, 2001, doi: 10.1109/7.913685.

[28] M. Elgendi, I. Norton, M. Brearley, D. Abbott, and D. Schuurmans, "Systolic peak detection in acceleration photoplethysmograms measured from emergency responders in tropical conditions," *PLoS One*, vol. 8, no. 10, p. e76585, 2013, doi: 10.1371/journal.pone.0076585.

[29] G. B. Moody and R. G. Mark, "The impact of the mit-bih arrhythmia database," *IEEE Eng. Med. Biol. Mag.*, vol. 20, no. 3, pp. 45–50, 2001, doi: 10.1109/51.932724.

[30] Y. Ichimaru and G. B. Moody, "Development of the polysomnographic database on CD-ROM," *Psychiatry Clin Neurosci.*, vol. 53, no. 2, pp. 175–177, 1999, doi: 10.1046/j.1440-1819.1999.00527.x.

[31] A. L. Goldberger, L. A. Amaral, L. Glass, J. M. Hausdorff, P. C. Ivanov, R. G. Mark, J. E. Mietus, G. B. Moody, C. K. Peng, and H. E. Stanley, "PhysioBank, PhysioToolkit, and PhysioNet: components of a new research resource for complex physiologic signals," *Circulation*, vol. 101, no. 23, pp. e215-e220, 2000, doi: 10.1161/01.CIR.101.23.e215.

[32] M. A. Pimentel, A. E. Johnson, P. H. Charlton, D. Birrenkott, P. J. Watkinson, L. Tarassenko, and D. A. Clifton, "Toward a robust estimation of respiratory rate from pulse oximeters," *IEEE Transactions on Biomedical Engineering*, vol. 64, no. 8, pp. 1914–1923, 2016, doi: 10.1109/TBME.2016.2613124.

[33] C. Orphanidou, S. Fleming, S. A. Shah, and L. Tarassenko, "Data fusion for estimating respiratory rate from a single-lead ecg," *Biomedical Signal Processing and Control*, vol. 8, no. 1, pp. 98-105, 2013, doi: 10.1016/j.bspc.2012.06.001.

[34] P. Langley, E. J. Bowers, and A. Murray, "Principal component analysis as a tool for analyzing beat-to-beat changes in ecg features: application to ecg-derived respiration," *IEEE transactions on biomedical engineering*, vol. 57, no. 4, pp. 821–829, 2009, doi: 10.1109/TBME.2009.2018297.

[35] D. Widjaja, C. Varon, A. Dorado, J. A. Suykens, and S. Van Huffel, "Application of kernel principal component analysis for single-lead-ecg-derived respiration," *IEEE Trans. Biomed. Eng.*, vol. 59, no. 4, pp. 1169–1176, 2012, doi: 10.1109/TBME.2012.2186448.

[36] H. X. Barnhart, M. J. Haber, and L. I. Lin, "An overview on assessing agreement with continuous measurements," *J. Biopharm. Stat.*, vol. 17, no. 4, pp. 529–569, 2007, doi: 10.1080/10543400701376480.

[37] C. J. Willmott and K. Matsuura, "Advantages of the mean absolute error (mae) over the root mean square error (rmse) in assessing average model performance," *Climate Res.*, vol. 30, no. 1, pp. 79–82, 2005, doi: 10.3354/cr030079.

APPENDIX. PATIENT-LEVEL RESULTS

Patient-level results for the proposed method on the MIT-BIH Polysomnographic and BIDMC databases are shown in Tables.VI and VII respectively. BR represents the mean of reference BR of each record. As described in section II-E, Q_{ECG}, Q_{PPG}, and Q_{BP} indicate the percentage of low quality windows. E_{ECG}, E_{BP}, and E_{PPG} indicate the MAPE for ECG, BP, and PPG signals respectively.

TABLE VI. Overall performance summary of methods applied to ECG or BP signals of the MIT-BIH Polysomnographic database.

Patients	Age	Sex	BR	Q_{BP}	E_{BP}	Q_{ECG}	E_{ECG}
SLP01a	44	M	12	0	1.1	0.1	1.3
SLP01b	44	M	12	0.7	2.5	0.1	3.6
SLP02a	38	M	23	12.4	8.3	1.3	2.5
SLP03	51	M	16	3.4	4.5	9.8	6.7
SLP04	40	M	10	1.0	3.1	5.1	3.7
SLP14	37	M	18	4.6	5.4	7.9	4.9
SLP16	33	M	24	13.9	8.9	10.4	5.3
SLP32	54	M	7	0.2	3.7	4.1	5.6
SLP37	39	M	15	0.1	5.5	0.7	4.2
SLP41	45	M	8	0.1	5.4	0	1.9
SLP45	42	M	14	0.2	6.2	5.3	4.9
SLP48	56	M	11	0	3.8	0.1	2.9
SLP59	41	M	13	4.6	7.4	0	3.5
SLP60	49	M	13	5.2	3.8	2.1	3.2
SLP61	32	M	21	0.1	4.0	0.9	4.2
SLP66	33	M	20	0.1	5.7	0	3.9
		Average:	14.8	2.9	5.0	3.0	3.9

TABLE VII. Overall performance summary of methods applied to ECG or PPG signals of the BIDMC database.

Patients	Age	Sex	BR	Q_{PPG}	E_{PPG}	Q_{ECG}	E_{ECG}
BIDMC01	88	M	24	9.4	7.2	0.2	3.1
BIDMC02	65	M	17	6.2	7.6	1.0	2.6
BIDMC03	46	F	17	4.8	5.4	1.2	3.5
BIDMC04	78	M	16	6.3	4.6	2.3	4.0
BIDMC05	73	F	7	3.5	3.8	0	2.1
BIDMC06	64	F	21	0.4	2.8	0.8	3.4
BIDMC07	74	F	20	0	1.4	0	1.8
BIDMC08	64	F	21	0.6	3.9	0	2.0
BIDMC09	64	F	20	1.3	4.1	0.9	3.3
BIDMC10	74	M	19	44.8	8.9	1.0	2.9
BIDMC11	50	M	24	31.1	9.5	0.2	3.1
BIDMC12	75	M	18	5.4	3.6	0	2.9
BIDMC13	71	F	24	12.6	7.0	0	1.9
BIDMC14	70	F	13	3.7	2.4	8.1	3.4
BIDMC15	51	M	14	9.3	3.9	0.2	3.1
BIDMC16	56	M	21	8.0	6.1	6.6	5.4
BIDMC17	72	F	22	3.5	3.3	0.2	3.7
BIDMC18	-	-	18	2.7	2.4	1.3	4.1
BIDMC19	85	F	14	7.5	4.7	0.8	2.9
BIDMC20	44	F	16	3.0	3.2	5.2	4.6
BIDMC21	44	F	15	6.9	5.9	2.3	3.8
BIDMC22	44	F	19	0.8	1.9	0	2.5
BIDMC23	44	F	19	23.6	8.7	8.9	4.9
BIDMC24	77	M	24	34.2	9.1	0.2	1.9
BIDMC25	74	F	16	25.0	8.3	19.7	5.2
BIDMC26	86	M	18	42.7	9.5	14.8	6.8
BIDMC27	43	M	11	4.8	2.8	2.9	3.1
BIDMC28	+90	M	18	37.1	9.2	1.5	4.0
BIDMC29	77	M	20	30.6	8.0	2.7	2.7
BIDMC30	48	F	18	14.3	6.4	1.3	1.9
BIDMC31	60	F	18	11.0	6.9	1.5	2.6
BIDMC32	+90	F	25	26.5	8.1	0	-
BIDMC33	76	F	14	39.8	8.7	12.4	6.6
BIDMC34	57	M	17	8.9	5.5	2.3	3.4
BIDMC35	67	F	19	41.1	9.1	2.5	3.7
BIDMC36	57	F	18	3.9	3.7	0.3	2.9
BIDMC37	70	F	17	7.6	4.2	0.7	3.0
BIDMC38	88	F	15	25.1	8.3	3.5	4.1
BIDMC39	88	F	15	19.8	7.9	0.4	2.6
BIDMC40	26	F	16	74.3	11.8	16.5	7.1
BIDMC41	73	F	14	19.4	7.7	1.3	4.5
BIDMC42	85	F	17	0	2.3	0.2	2.8
BIDMC43	19	F	17	13.1	6.1	0.2	3.3
BIDMC44	+90	F	18	27.6	8.9	1.0	4.5
BIDMC45	52	M	15	13.9	4.5	0.8	3.8
BIDMC46	61	F	13	24.1	9.3	13.9	6.4
BIDMC47	48	M	23	15.3	6.5	6.2	3.1
BIDMC48	37	M	13	27.7	7.2	3.9	4.2
BIDMC49	77	M	16	58.1	9.8	0.7	2.3
BIDMC50	67	M	16	4.0	3.1	0.2	1.9
BIDMC51	78	F	18	0	1.7	0	2.5
BIDMC52	29	F	20	6.1	4.2	27.9	8.5
BIDMC53	81	M	23	13.2	5.8	4.3	3.6
		Average:	17.8	16.3	6.0	3.5	3.6

ALI ADAMI was born in Yazd, Iran, in 1993. He received the B.Sc. degree in Electrical Engineering from Hamedan University of Technology, Hamedan, Iran, in 2016 and the M.Sc. degree in Biomedical Engineering from Shiraz University, Shiraz, Iran, in 2019.

His research interests include statistical signal processing and time-frequency analysis of biomedical recordings, and he is working on the modeling and analysis of physiological signals and the cardiovascular system.

REZA BOOSTANI was born in 1973. He received the B.Sc. degree in Electrical Engineering from Shiraz University, Shiraz, Iran, in 1996, and the M.Sc. and Ph.D. degrees in Biomedical Engineering from the Amirkabir University of Technology, Tehran, Iran, in 1999 and 2004, respectively.

He has spent his research period in the Graz University of Technology in the BCI field from 2003 to 2004. Since 2005, he has been a Faculty Member with the Computer Science and Engineering Department, Shiraz University. His current research interests include biomedical signal processing, statistical pattern recognition, and machine learning.

FAEZEH MARZBANRAD received her B. Sc. and M. Sc. degrees in electrical engineering from Shiraz University, Shiraz, Iran, in 2007 and 2010, respectively and her PhD from University of Melbourne, Melbourne, Australia in 2016. She is currently a lecturer, in the department of electrical and computer systems engineering, Monash University, Australia. Her research interests include biomedical signal processing, machine learning, low-cost medical devices and Mobile-Health.

PETER H. CHARLTON received the M.Eng. degree in Engineering Science from the University of Oxford, Oxford, UK, in 2010 and the Ph.D. degree from King's College London, London, UK, in 2017.

From 2010 to 2020 he conducted his research at King's College London, developing techniques to continuously monitor respiratory and cardio-vascular health using wearable sensors. His Ph.D. focused on using signal processing and machine learning techniques to identify acute deteriorations in hospital patients. In 2020, Peter was awarded a British Heart Foundation fellowship to develop techniques to use clinical and consumer devices to enhance screening for atrial fibrillation, held at the University of Cambridge, Cambridge, UK.

• • •